SSNP133 - Cracking of a plate perforated with the cohesive models

Abstract:

This test makes it possible to model the propagation of two cracks in an elastic perforated plate.

Modelization A : Elements of joint, cohesive model CZM_LIN_REG
Modelization B : Elements with internal discontinuity, cohesive model CZM_EXP.
Modelization C : Elements of interface, cohesive model CZM_OUV_MIX
Modelization D : Elements of joint, cohesive model CZM_EXP_REG
Modelization E : Modelization XFEM, cohesive model CZM_EXP_REG. Mesh conforms to cracks.
Modelization F : Modelization XFEM, cohesive model CZM_EXP_REG. Mesh triangles nonin conformity.
Modelization G : Modelization XFEM, cohesive model CZM_EXP_REG. Mesh not structured.
Modelization H : Modelization XFEM, cohesive model CZM_LIN_REG. Mesh conforms to cracks.
Modelization I : Modelization XFEM, cohesive model CZM_OUV_MIX. Mesh conforms to cracks.
Modelization J : Modelization XFEM, cohesive model CZM_OUV_MIX. Mesh nonin conformity.

The classification local *ad hoc* of the cohesive elements (except $X-FEM$) is assured by the command MODI_MAILLAGE and key word ORIE_FISSURE. The brutal opening of cracks is ensured by the control of the loading available for each one of these models (see [R7.02.11]).

1 Problem of reference

1.1 Geometry and loading

One considers a square plate on side $2000\,mm$ with a hole of radius $R=500\,mm$ centered in the vertical direction and decentred in the horizontal direction (see Figure 1.1-a). The plate admits a horizontal symmetry plane (AB') passing by the center of hole. This symmetry can enable us to reduce our study to the higher half of the plate when that is possible.

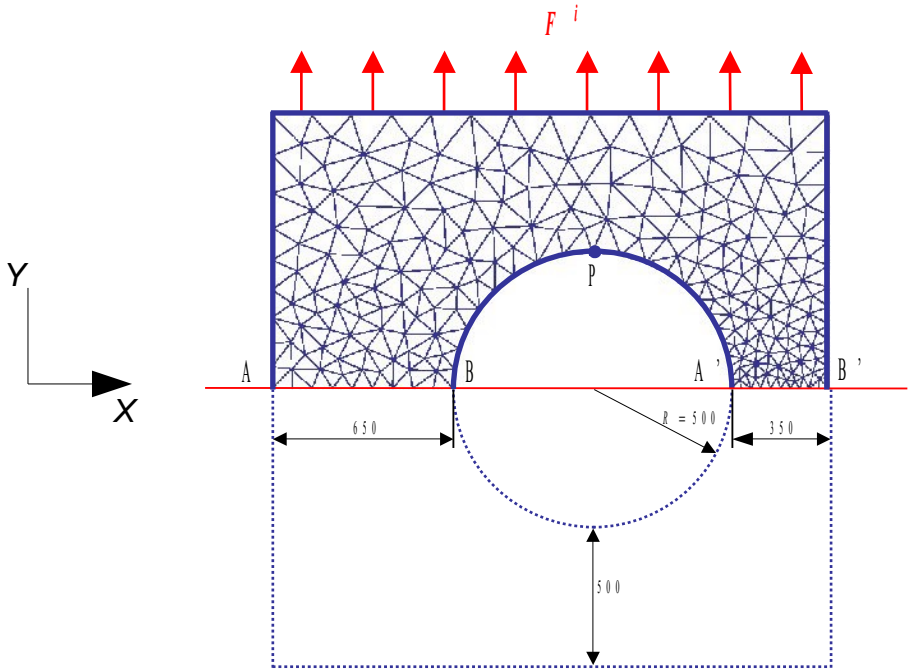

Figure 1.1-a : Diagram of the perforated plate, boundary conditions and loading.

It is considered *a priori* that the cracks will develop along the axis of symmetry on both sides of hole. One thus lays out the cohesive elements along the ways $[AB]$ and $[A'B']$. The loading consists in applying one density of unit surface F^i force directed in the direction Y to the upper part of the field. The intensity of this force will be given by the control of the loading (see [R7.02.11]). In addition, one imposes conditions of symmetry (null displacements according to Y) on the lower face of the cohesive elements. Lastly, one blocks rigid body motions by imposing a following null displacement X on the point P, top of hole.

For the modelizations E with J, we have a X-FEM formulation: it is then necessary to model whole structure for the moment. One introduces an interface on the line (AB'). One points out the approximation of the field of displacement for the nodes whose support is intersected by an interface XFEM:

$$\boldsymbol{u}_h(\boldsymbol{x})=\sum_i \phi_i(\boldsymbol{x})\boldsymbol{a}_i+\sum_i \phi_i(\boldsymbol{x})\boldsymbol{b}_i H\left(lsn(\boldsymbol{x})\right)$$

In order to block rigid body motions, it is wished that the interface be an axis of symmetry for the problem. If one considers M^+ and M^- of the points located immediately at the top and the lower part of the interface, we want that $u_y(M^+)+u_y(M^-)=0$.
For an interface in conformity, this implies $a_y=0$ on the nodes of the interface (figure 1.1-a).

For an interface NON-in conformity which intersects the edges in their medium, by noting N_{SUP} and the N_{INF} nodes in with respect to share and of other of crack (figure 1.1-b), this implies:

$$a_y(N_{\text{SUP}})+a_y(N_{\text{INF}})=0$$

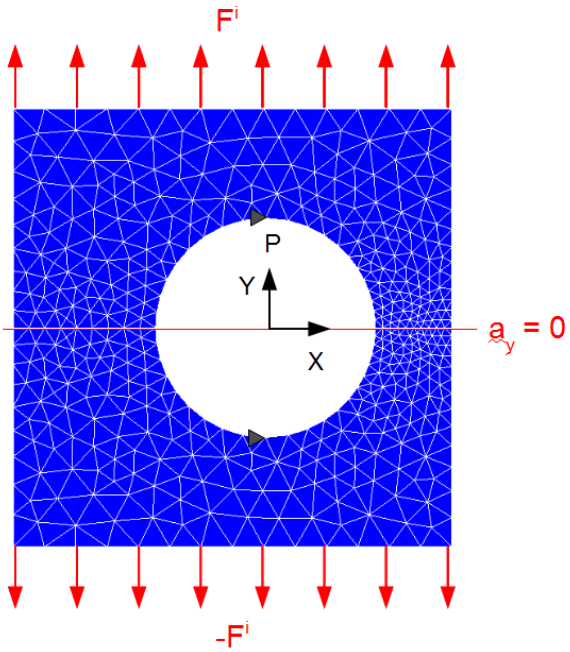

Appear 1.1-a: loading with a crack conforms.

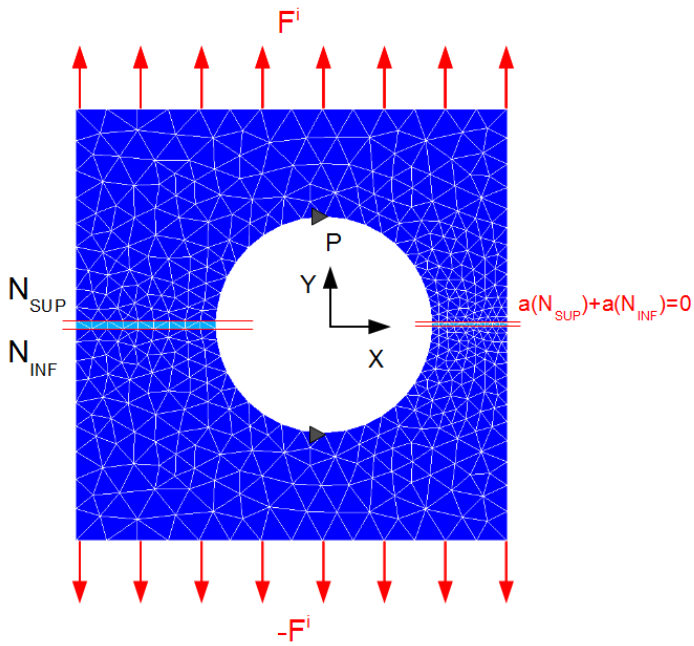

Appear 1.1-b: loading for a crack NON-in conformity.

1.2 Properties material

the values of the Young modulus, the Poisson's ratio, the critical stress and the tenacity of the material are in the following way selected:

$$E=30000\,MPa \quad \nu=0.2 \quad \sigma_c=0.2\,MPa$$

$$G_c=100\,Pa.mm \quad \Rightarrow \quad \text{problème symétrisé}$$

$$G_c=200\,Pa.mm \quad \Rightarrow \quad \text{problème non symétrisé}$$

They are values “tests” which do not correspond to any material in particular. The purpose of the choice of the cohesive parameters is obtaining a solution with a relatively coarse mesh. One recalls that to ensure a correct solution (accuracy and good convergence) with these models, it is necessary that there are several elements in the cohesive zone (see Doc. [U2.05.07]).

Note:

When the mechanical problem is symmetrized, one models only half of the cracks (only one lip). These last dissipate an energy twice less important than if one had modelled the plate entirely.

To model a material of tenacity given G_c, it is thus necessary to carry out simulation with a value of $G_c/2$.

2 Reference solution

It does not have there a reference solution for this problem. One thus carries out tests of non regression. It is checked that the tests $XFEM$ give the same results as their counterparts FEM. For this reason, the modelization D constitutes a reference for the modelizations E to G, the modelization A constitutes a reference for the modelization H and the modelization C constitutes a reference for the modelizations I and J.

3 Modelization A

3.1 Characteristic of the modelization

the simulation of the propagation of cracks by brittle fracture is carried out with the modelization PLAN_JOINT and constitutive law CZM_LIN_REG for the meshes cohesive ones. The voluminal elements, in plane strains D_PLAN, are elastic.

3.2 Characteristics of the mesh

One carries out a linear mesh not structured of the perforated half-plate and potential crack.
Voluminal elements (DCB): 404 TRIA3
Elements of joint (crack way): 19 QUAD4

3.3 Quantities tested and results

One carries out tests of non regression on the total response: F^i resultant of the force imposed on the upper face *versus* U displacement of the node P on the top of hole.

Quantity tested	*Code_Aster*	*Tolerance (%)*
U at time 50	3.3166D-03	0.10
F at time 50	4.26153D+07	0.10
U at time 100	1.29488D-03	0.10
F at time 100	2.73873D+06	0.10
U at time 150	6.45752D-03	0.10
F at time 150	7.87206D+06	0.10
U at time 200	1.04754D-02	0.10
F at time 200	2.16189D+06	0.10

4 Modelization B

4.1 Characteristic of the modelization

the simulation of the propagation of cracks by brittle fracture is carried out with the modelization PLAN_ELDI and constitutive law CZM_EXP for the meshes cohesive ones. The voluminal elements, in plane strains D_PLAN, are elastic.

4.2 Characteristics of the mesh

One carries out a linear mesh not structured of the perforated half-plate and potential crack.
Voluminal elements (DCB): 404 TRIA3
Elements with internal discontinuity (crack way): 19 QUAD4

4.3 Quantities tested and results

One carries out tests of non regression on the total response: F^i resulting from the force imposed on the upper face *versus* U displacement of the node P at the top of hole.

Quantity tested	*Code_Aster*	*Tolerance (%)*
U at time 50	3.60651D-03	0.10
F at time 50	5.78832D+07	0.10
U at time 75	3.54604D-03	0.10
F at time 75	5.11117D+07	0.10
U at time 100	3.39435D-03	0.10
F at time 100	4.43684D+07	0.10
U at time 159	4.32977D-03	0.10
F at time 159	1.001265D+07	0.10

5 Modelization C

5.1 Characteristic of the modelization

the simulation of the propagation of cracks by brittle fracture is carried out with the modelization PLAN_INTERFACE and constitutive law CZM_OUV_MIX for the meshes cohesive ones. The voluminal elements, in plane strains D_PLAN, are elastic.

5.2 Characteristics of the mesh

One carries out a quadratic mesh not structured of the perforated half-plate and potential crack.
Voluminal elements (DCB): 404 TRIA6
Elements of interface (crack way): 19 QUAD8

5.3 Quantities tested and results

One carries out tests of non regression on the total response: F^i resulting from the force imposed on the upper face versus U displacement of the node P at the top of hole.

Quantity tested	Code_Aster	Tolerance (%)
U at time 50	2.87853E-03	0.10
F at time 50	2.88263E+07	0.10
U at time 75	6.55609E-03	0.10
F at time 75	1.04922E+07	0.10
U at time 100	7.47879E-03	0.10
F at time 100	4.94452E+06	0.10
U at time 140	0.0157679	0.10
F at time 140	8.56080E+05	0.10

6 Modelization D

6.1 Characteristic of the modelization D

the simulation of the propagation of cracks by brittle fracture is carried out with the modelization PLAN_JOINT and constitutive law CZM_EXP_REG for the meshes cohesive ones. The voluminal elements, in plane strains D_PLAN, are elastic.

6.2 Characteristics of the mesh

One carries out a linear mesh not structured of the perforated half-plate and potential crack.
Voluminal elements (DCB): 804 TRIA3
Elements of joint (crack way): 19 QUAD4

6.3 Quantities tested and results

One carries out tests of non regression on the total response: F^i resulting from the force imposed on the upper face versus U displacement of the node P at the top of hole.

Quantity tested	Code_Aster	Tolerance (%)
U at time 50	3.32215D-03	0.10
F at time 50	4.21054D+07	0.10
U at time 100	2.52359D-03	0.10
F at time 100	5.3546D+06	0.10
U at time 150	7.09118D-03	0.10
F at time 150	6.75039D+06	0.10

One sees that the penalization of the cohesive model introduces a light difference between the results. If we thus compare the results of the modelization D with those of B, we have the curved force-displacement of the figure 6.3-a.

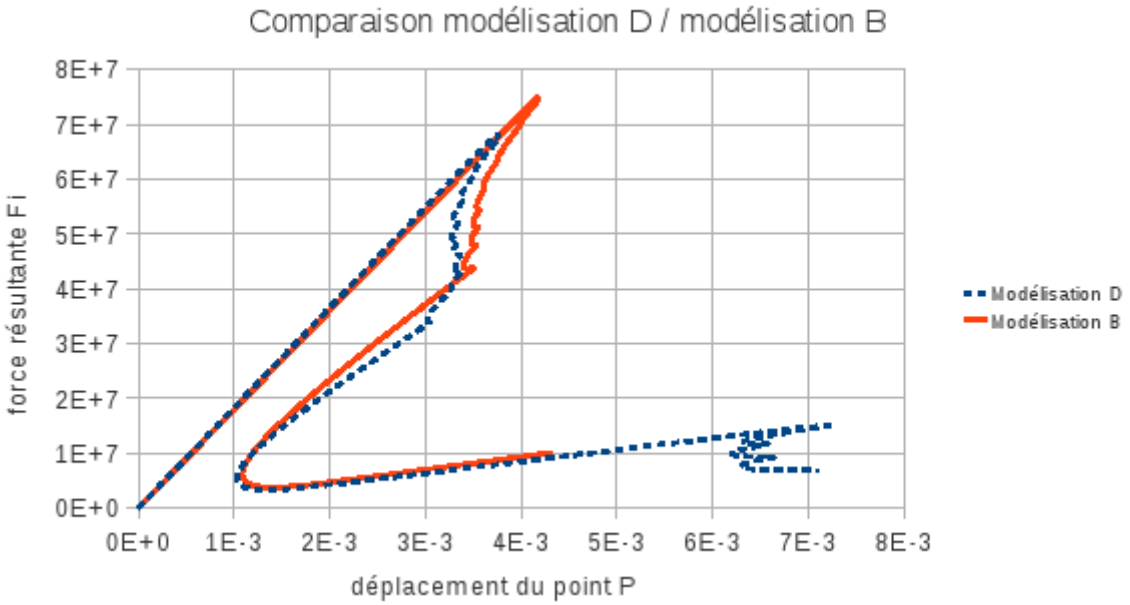

Appear 6.3-a: comparison elements of joint with elements to internal discontinuity.

7 Modelization E

7.1 Characteristic of the modelization E

an interface of equation $\left[Y=0\right]$ is introduced into the model using a formulation XFEM, via a level set norm. The simulation of the propagation of cracks by brittle fracture is carried out thanks to a relation of the type CZM_EXP_REG between stress and jump of displacement between the lips of the interface. Syntactically, this relation is included in the definition of a contact zone between the two lips of crack, with integration FPG3 or FPG2 and in formulation CZM. This means that the contact is managed by the cohesive model and that there is no friction. Physically, we find ourselves then rigorously in the same situation as the modelization D. The voluminal elements, in plane strains D_PLAN, are elastic.

7.2 Characteristics of the mesh

One carries out a mesh of the plate perforated in conformity with crack.
Voluminal elements (DCB): 804 TRI3

7.3 Quantities tested and results

The modelization D are used as reference. One sees on the figure 7.3-a that the results are perfectly superposable.

Quantity tested	*Standard of Reference*	*Code_Aster*	*Tolerance (%)*
U to time 50	AUTRE_ASTER	3.32215D-03	0.10
F at time 50	AUTRE_ASTER	4.21054D+07	0.10
U at time 100	AUTRE_ASTER	2.52359D-03	0.10
F at time 100	AUTRE_ASTER	5.3546D+06	0.10
U at time 150	AUTRE_ASTER	7.09118D-03	0.10
F at time 150	AUTRE_ASTER	6.75039D+06	0.10

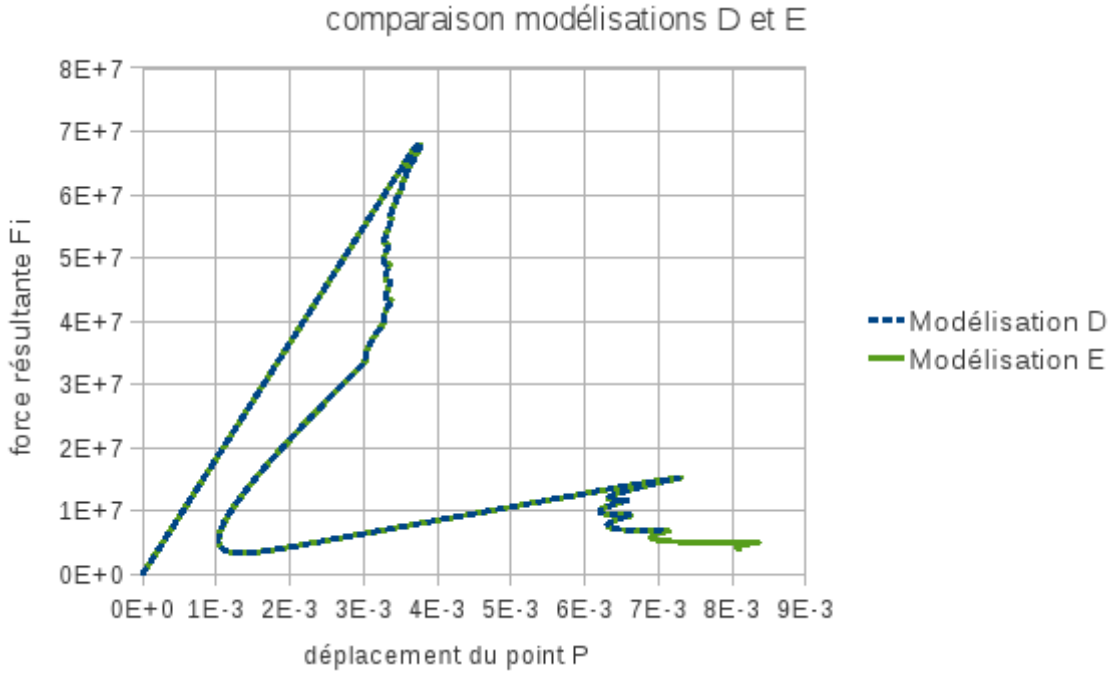

Figure 7.3-a: adequacy of the modelization D with the modelization E

7.4 Comments

the solutions FEM are superposable with the solutions $XFEM$ which have the same cohesive model. Consequently, this test makes it possible to validate the implementation $XFEM$ of the cohesive model, like that of control by elastic prediction.

8 Modelization F

8.1 Characteristic of the modelization F

the characteristics of the modelization are strictly identical to the modelization E. Only the mesh differs.

8.2 Characteristics of the mesh

One carries out a mesh of the plate entirely triangular, NON-in conformity with crack, such as certain intersected edges are nonvital.
Voluminal elements (DCB): 842 `TRI3`

8.3 Quantities tested and results

the beginning of computation requires a little more subdivisions than the modelization E. Taking into account this difference in the sequences in subdivision, the results of the modelizations E and F slightly different are compared urgent per time. On the other hand, one sees on the figure 8.3-a that they are superposable. Having proven this correspondence, one thus takes for value of reference of non regression those of the modelization F.

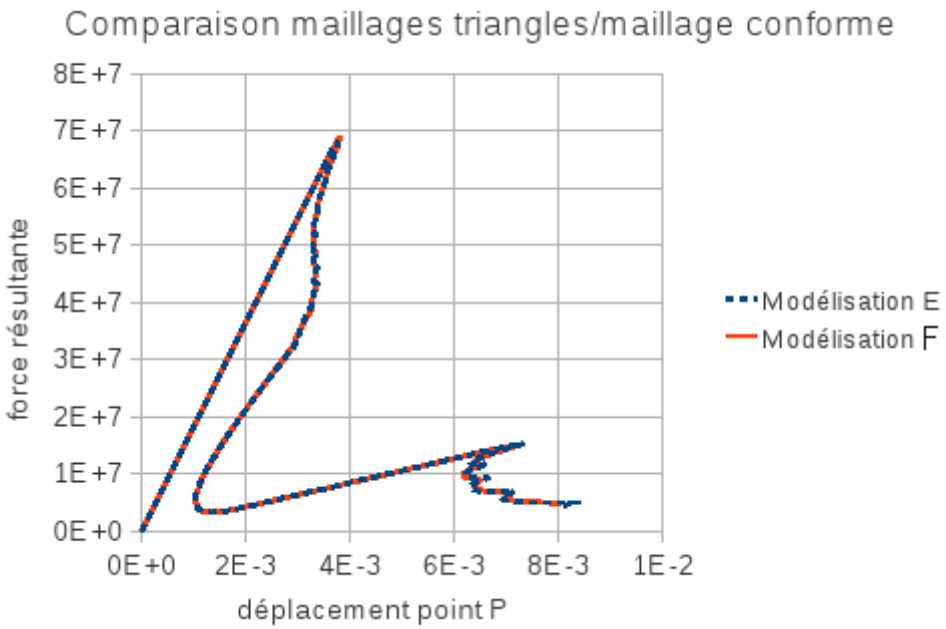

Appear 8.3-a: Comparison mesh triangles/mesh conforms

Quantity tested	Standard of reference	Code_Aster	Tolerance (%)
U to time 50	NON_REGRESSION	3.34481D-03	0.10
F at time 50	NON_REGRESSION	4.26501D+07	0.10
U at time 100	NON_REGRESSION	2.28519D-03	0.10
F at time 100	NON_REGRESSION	4.85041D+06	0.10
U at time 150	NON_REGRESSION	6.83775D-03	0.10
F at time 150	NON_REGRESSION	6.86061D+06	0.10

9 Modelization G

9.1 Characteristic of the modelization G

the characteristics of the modelization are strictly identical to the modelization E. Only the mesh differs.

9.2 Characteristics of the mesh

One carries out a mesh of the entirely triangular plate, not regulated. Certain edges are in conformity with crack. Some are intersected.
Voluminal elements (DCB): 698 TRI3

9.3 Results of the modelization G

One obtain one result slightly different from the modelization D. This is unlike mesh between the two modelizations. Small the snap-backs is of origin numerical and related to the refinement of the mesh. They are larger here because the mesh is refined less (fig.9.3-a9.3-a). One thus changes the values of reference for the same reasons as the modelization F.

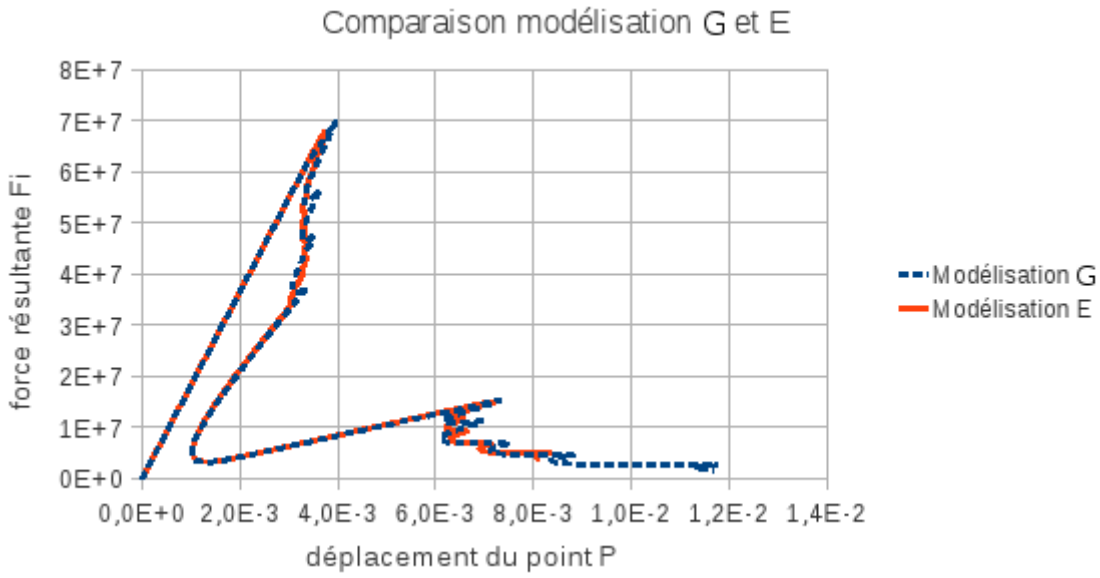

Appear 9.3-a: comparison between modelizations G and E

Quantity tested	*Standard of reference*	*Code_Aster*	*Tolerance (%)*
U at time 50	NON_REGRESSION	3.21777D-03	0.10
F time 50	NON_REGRESSION	3.6512D+07	0.10
U time 100	NON_REGRESSION	7.41292D-03	0.10
F time 100	NON_REGRESSION	1.54984D+07	0.10
U time 150	NON_REGRESSION	7.76637D-03	0.10
F time 150	NON_REGRESSION	4.65793D+06	0.10

10 Modelization H

10.1 Characteristic of the modelization H

L are characteristic of the modelization are strictly identical to those of the modelization E . Only the cohesive model differs: model CZM_LIN_REG is used.

10.2 Characteristics of the mesh

The mesh is the same one as that of the modelization E . Let us recall that it is in conformity with crack.
Voluminal elements (DCB): 804 TRI3.

10.3 Results of the modelization H

The modelization A is used as reference. The results are perfectly superposable.

Quantity tested	*Standard of reference*	*Code_Aster*	*Tolerance (%)*
U to time 50	AUTRE_ASTER	3.3166D-03	0.10
F at time 50	AUTRE_ASTER	4.26153D+07	0.10
U at time 100	AUTRE_ASTER	1.29488D-03	0.10
F at time 100	AUTRE_ASTER	2.73873D+06	0.10
U at time 150	AUTRE_ASTER	6.45752D-03	0.10
F at time 150	AUTRE_ASTER	7.87206D+06	0.10

11 Modelization I

11.1 Characteristic of the modelization I

the characteristics of the modelization E are taken again, except for the cohesive model. One uses mixed model CZM_OUV_MIX. Consequently, the mesh of the modelization E is made quadratic, and one P2P1 defines in operator MODI_MODELE_XFEM a discretization for the contact.

11.2 Characteristics of the mesh

The mesh is the same one as that of the modelization E. Let us recall that it is in conformity with crack.
Voluminal elements : 804 SORT 6.

11.3 Results of the modelization I

The modelization C is used as reference. The layouts of the responses for the two modelizations are perfectly superposable.

Quantity tested	*Code_Aster*	*Tolerance (%)*
U at time 50	2.8872E-03	0.10
F at time 50	2.8603E+07	0.10
U at time 75	6.43269E-03	0.10
F at time 75	9.8916E+06	0.10
U at time 100	7.8109E-03	0.10
F at time 100	4.7092E+06	0.10
U at time 140	2.2116E-02	0.10
F at time 140	6.24908E+05	0.10

12 Modelization J

12.1 Characteristic of the modelization J

the characteristics of the modelization are strictly identical to the modelization I. Only the mesh differs.

12.2 Characteristics of the mesh

One carries out a mesh of the entirely triangular plate, not regulated. Certain edges are in conformity with crack. Some are intersected.
Voluminal elements (DCB): 698 TRI6.

12.3 Results of the modelization J

One obtains one result slightly different from the modelization I. This is unlike mesh between the two modelizations. Small the snap-backs is of origin numerical and related to the refinement of the mesh. They are larger here because the mesh is refined less. One thus changes the values of reference.

Quantity tested	*Standard of reference*	*Code_Aster*	*Tolerance (%)*
U at time 50	NON_REGRESSION	2.9189E-03	0.10
F at time 50	NON_REGRESSION	2.9439E+07	0.10
U at time 75	NON_REGRESSION	6.6043E-03	0.10
F at time 75	NON_REGRESSION	1.0854E+07	0.10
U at time 100	NON_REGRESSION	7.2936E-03	0.10
F at time 100	NON_REGRESSION	5.2103E+06	0.10
U at time 140	NON_REGRESSION	0.014454	0.10
F at time 140	NON_REGRESSION	9.5855E+05	0.10

13 Summary of the results

the cohesive models make it possible qualitatively to simulate the brutal propagation of two cracks in brittle fracture through a perforated plate. The total responses of the seven models (in terms of force-displacement) are appreciably the same ones. The control of the loading makes it possible to follow the brutal fracture of the two ligaments on both sides of hole, leading to two “back return” in the total response.